Available online at www.sciencedirect.com

ScienceDirect

Nuclear Physics A 932 (2014) 189–196

NUCLEAR PHYSICS A

www.elsevier.com/locate/nuclphysa

Jet production and structure in pp, p–Pb and Pb–Pb collisions measured by ALICE

Rosi Reed for the ALICE Collaboration

Received 24 April 2014; received in revised form 15 October 2014; accepted 15 October 2014

Available online 22 October 2014

Abstract

In ultra-relativistic heavy-ion collisions a hot, dense medium of strongly interacting matter called the Quark Gluon Plasma (QGP) is formed. One of the main goals of jet measurements is to study how the fragmentation of hard scattered partons is modified as they traverse the medium. A study of jet spectra and correlations in a variety of colliding systems will allow a better understanding of the detailed mechanisms of the in-medium energy loss and will further constrain theoretical models for this process. This work will report the recent ALICE results on jet production, di-jet acoplanarity k_{T} and hadron + jet correlations in pp, p–Pb and Pb–Pb collisions and discuss their sensitivity to a modified jet fragmentation function.

Keywords: Jets; Cold nuclear matter; Hot nuclear matter; Jet quenching

1. Introduction

One of the goals of colliding heavy-ion collisions is to investigate how partons lose energy in the Quark Gluon Plasma (QGP) that is formed in these collisions. Jets, formed when a hard-scattered parton fragments into a collimated spray of hadrons, are a well suited probe of the medium as the initial hard scatter of the parton occurs prior to QGP formation. The partons then propagate through the medium, and lose energy due to in-medium interactions, and then fragment into jets. The modification of jets due to this interaction with the medium is called jet quenching [1]. Currently at the LHC we have three different collisional systems available for analysis: pp, p–Pb and Pb–Pb, which allow us to investigate jets from hard QCD processes as a baseline, and see how these jets are modified due to cold and hot nuclear matter effects.

E-mail address: rosi.reed@wayne.edu.

http://dx.doi.org/10.1016/j.nuclphysa.2014.10.048

2. Experimental set-up

The results reported in this proceedings are from data collected by the ALICE experiment in 2010 and 2011 at energies of 2.76 (pp and Pb–Pb), 5.02 (p–Pb), and 7 TeV (pp) per nucleon pair. Tracks from charged particles are reconstructed with the Time Projection Chamber (TPC) and the Inner Tracking System (ITS), a six-layer silicon detector which provides a precise measurement of the primary vertex together with the first reconstructed points of the tracks, down to a transverse momentum (p_{T}) of 0.15 GeV/c. The Silicon Pixel Detector (SPD), the two inner layers of the ITS, which has an acceptance in pseudorapidity of $|\eta| < 1.4$, is also used in order to select high quality tracks which correspond to the primary collisions. Tracks are reconstructed at mid-rapidity ($|\eta| < 0.9$) and in full azimuth. The Electromagnetic Calorimeter (EMCal), a Pb-scintillator sampling calorimeter measures energy from neutral particles that interact electromagnetically, mainly photons and π^0s, down to a cluster energy of 0.30 GeV. The EMCal covers mid-rapidity $|\eta| < 0.7$ and the azimuth with an acceptance of $\Delta\phi = 100°$. The ALICE VZERO scintillator detectors, which cover $2.8 < \eta < 5.1$ and $-3.7 < \eta < -1.7$, are used to determine the event centrality in Pb–Pb and p–Pb events by measuring the forward particle multiplicity. The VZEROs are also used to define the minimum-bias interaction trigger and, in the case of Pb–Pb, to enhance the sample of central events based on the forward multiplicity of the event. For a complete description of the ALICE detector see Ref. [2].

3. Jets in ALICE

The jets measured by ALICE detector are placed into two categories: charged jets and full jets. The former are jets that are reconstructed from charged particles only measured with the ALICE tracking system. These jets are corrected for effects such as the tracking efficiency and resolution based on the simulations of jets with PYTHIA [12,13] and the detector response with GEANT, but they are not corrected for the unmeasured neutral component. Full jets, which we will simply refer to as jets for the rest of this proceedings, include the neutral energy component that is measured with the EMCal, and these are corrected for all missing energy effects similarly as done for charged jets.

The collection of tracks and corrected EMCal clusters were assembled into jets using the anti-k_{T} or the k_{T} algorithms [3–6] with a resolution parameter of $R = 0.2$–0.6. Only those jets that were at least R away from the acceptance boundaries of the TPC or EMCal were used in the analyses described here. The jets found by the anti-k_{T} algorithm were used to determine the signal jets in the pp, p–Pb and Pb–Pb analyses, the jets found by the k_{T} algorithm were used to quantify the underlying event density in the p–Pb and Pb–Pb analyses.

4. Results from pp

Jet measurements in pp collisions are needed as a baseline in order to fully quantify the modification of the jet spectrum in heavy-ion collisions due to the presence of the hot and dense QGP medium. Two important baseline measurements are the differential cross-section in $\sqrt{s} = 2.76$ TeV and the charged jet cross section ratio at $\sqrt{s} = 7$ TeV. In this analysis the measured jets were corrected back to the particle level utilizing a simulation based bin-by-bin technique where the simulated events were generated by PYTHIA and the detector response was simulated by GEANT. In this analysis, the jet energy shift was approximately 20% with an uncertainty less than 4% [7]. Fig. 1 shows the inclusive differential jet cross section obtained with

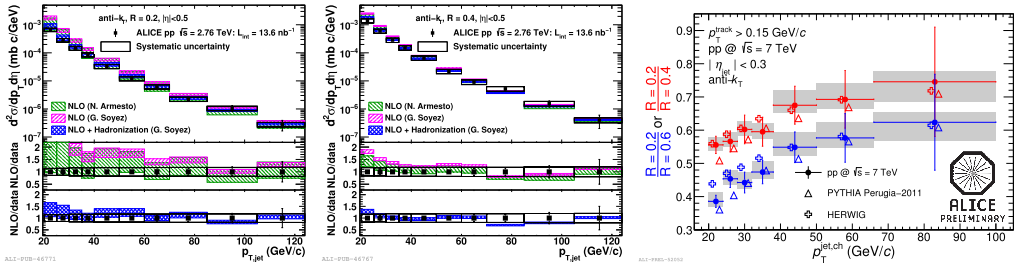

Fig. 1. The solid squares indicate the inclusive full jet differential cross section obtained with resolution parameters $R = 0.2$ (left) and $R = 0.4$ (middle) measured in pp collisions at 2.76 TeV data [7]. The empty boxes are systematic uncertainties on the cross-section. The left and right hashed boxes indicate the NLO calculations without hadronization, while the cross-hashed boxes indicate the NLO calculation with hadronization (color online). In contrast, the plot on the right, the solid points are the ratios jet production rates of $R = 0.2/R = 0.4$ in red (upper points) and $R = 0.2/R = 0.6$ in blue (lower points) for charged jets measured at $\sqrt{s_{\mathrm{NN}}} = 7$ TeV. The shaded boxes indicate the systematic uncertainty on the ratio. In the open triangles are the points from PYTHIA and in open crosses are points from HERWIG [8].

$R = 0.2$ and $R = 0.4$ compared to a pQCD calculation at NLO with and without hadronization effects [7]. The calculations agree well with the measured spectrum once hadronization is incorporated, which indicates that the process of jet formation is well understood. Additional analysis details can be found in [7].

The ratio of jet cross sections with different resolution parameters has some sensitivity to the underlying jet structure. The ratio of the differential cross-sections shown in Fig. 1 was reported in [7] for $\sqrt{s_{\mathrm{NN}}} = 2.76$ TeV. This ratio can be compared to the ratio in p–Pb or Pb–Pb events. In Fig. 1, the ratios of $R = 0.2$ over $R = 0.4$ or 0.6 for charged jets at mid-rapidity at a collision energy of $\sqrt{s_{\mathrm{NN}}} = 7$ TeV are shown. These ratios are compared to the same values from PYTHIA and HERWIG simulated events [8]. There is good agreement between data and simulation above 30 GeV/c, below this PYTHIA tends to underpredict the data for both the ratios and HERWIG tends to overpredict the data for the ratio $R = 0.2/R = 0.6$. The 7 TeV data is an important baseline for the 5.02 TeV p–Pb results as it is the pp reference with the closest energy.

5. Results from p–Pb

By analyzing collisions of protons on lead, Cold Nuclear Matter (CNM) effects such as shadowing, k_{T} broadening, or the nuclear modification of the PDF can be quantified. The results in this proceedings use the data from p–Pb collisions at an energy of $\sqrt{s_{\mathrm{NN}}} = 5.02$ TeV from data taken in the first months of 2013. The analyses presented in this proceeding use minimum-bias and jet-patch triggers. The event samples were divided into several multiplicity event classes [9]. These event classes are fractions of the total event sample, defined by the total charge deposited in the VZERO-A detector, which is located in the lead going direction at $2.8 < \eta < 5.1$. The multiplicity classes used in the following analyses were: 0–20%, 20–40%, 40–100% and 0–100% (minimum-bias).

5.1. R_{pPb}

The background is calculated event-by-event and subtracted jet-by-jet. The distribution of the regional fluctuations around the mean background density value is evaluated by the Random Cone (RC) approach where the δp_{T} distribution is calculated event-by-event by randomly throw-

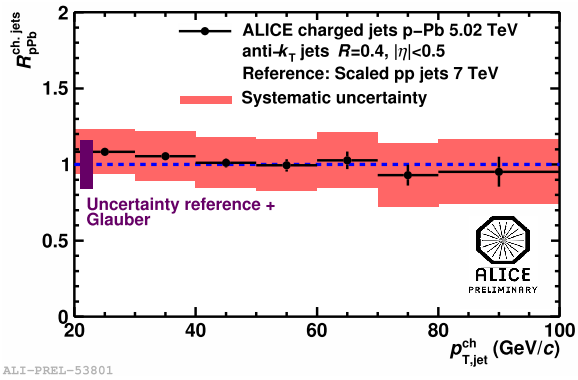

Fig. 2. The solid circles show the R_{pPb} as a function of $p_{\mathrm{T,\,jet}}^{\mathrm{ch}}$ for $R = 0.4$ charged jets in minimum-bias p–Pb collisions at $\sqrt{s_{\mathrm{NN}}} = 5.02$ TeV. The reference used was the measured spectrum from pp collisions at $\sqrt{s_{\mathrm{NN}}} = 7$ TeV scaled by PYTHIA. The solid boxes around the points are the systematic uncertainties from the detector effects, background fluctuations and unfolding. Uncertainties in the reference and the Glauber model are shown as a small box about $R_{\mathrm{pPb}} = 1$ [11].

ing a cone with the same radius as the resolution parameter used for the jet finding algorithm into the acceptance and calculating $\delta p_{\mathrm{T}} = \Sigma p_{\mathrm{T}} - \rho\pi R^2$. The measured spectrum is corrected for background fluctuations and detector effects using an unfolding technique with a response matrix based on the measured δp_{T} distributions, and detector response from PYTHIA + GEANT simulations.

Fig. 2 shows the nuclear modification factor, R_{pPb}, from minimum-bias p–Pb collisions as a measure for cold nuclear matter effects where it is calculated as $R_{\mathrm{pPb}}(p_{\mathrm{T}}) = \frac{dN_{\mathrm{pPb}}/dp_{\mathrm{T}}}{\langle T_{\mathrm{pPb}}\rangle d\sigma_{\mathrm{pp}}/dp_{\mathrm{T}}}$. The nuclear overlap function, T_{pPb}, is related to the number of binary collisions via $\langle N_{coll}\rangle = \langle T_{\mathrm{pPb}}\rangle \sigma_{\mathrm{inelastic\,pp}}$, where the number of binary collisions was calculated using the Glauber model [10]. Since we do not have pp data at $\sqrt{s_{\mathrm{NN}}} = 5.02$ TeV the reference was created by scaling the measured charged jet spectrum from 7 TeV using a bin-by-bin factor calculated with PYTHIA. The resulting R_{pPb} is consistent with unity, which indicates that there is no large CNM effect on the jet spectrum in p–Pb collisions [11].

5.2. *Dijet* k_{T}

To select charged dijet pairs, each measured charged jet is correlated with the leading charged jet in the opposite hemisphere. The angle between the dijet pair, $\Delta\phi_{\mathrm{ch,\,dijet}}$, is required to fulfill $|\Delta\phi_{\mathrm{ch,\,dijet}} - \pi| < \pi/3$. The azimuthal acoplanarity of dijet production is studied by measuring the transverse component of the k_{T} vector of the dijet system, defined as: $k_{\mathrm{T}} = p_{\mathrm{T,\,jet}}^{\mathrm{ch}} \sin(\Delta\phi_{\mathrm{ch,\,dijet}})$. In the minimum bias events, charged jets with $p_{\mathrm{T,\,jet}}^{\mathrm{ch}} > 20$ GeV/c are considered, while in the triggered data the requirement was increased to $p_{\mathrm{T,\,jet}}^{\mathrm{ch}} > 40$ GeV/c or $p_{\mathrm{T,\,jet}}^{\mathrm{ch}} > 60$ GeV/c, depending on the trigger threshold used.

Since k_{T} is a symmetric distribution around zero, the value $|k_{\mathrm{T}}|$ is reported. The measurements are compared to PYTHIA predictions to determine whether there is k_{T} broadening in p–Pb collisions [12,13]. The measured $|k_{\mathrm{T}}|$ distributions are corrected for background fluctuations and detector effects by applying bin-by-bin correction factors. Fig. 3 shows the corrected $|k_{\mathrm{T}}|$ distributions for several kinematic intervals for the trigger jet in the 0–20% V0A multiplicity class. The associated charged jet has a minimum $p_{\mathrm{T,ch\,jet}}$ of 20 GeV/c and always has a lower

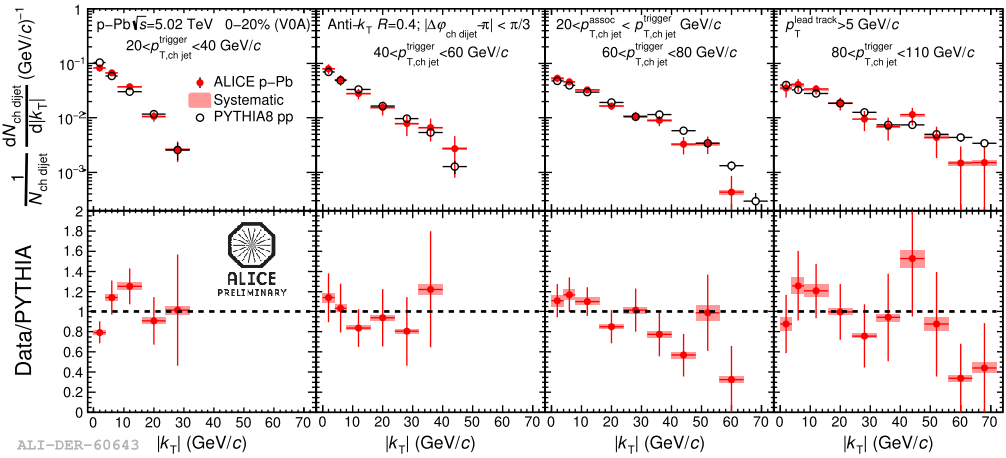

Fig. 3. The top row of panels shows the $R = 0.4$ di-jet $|k_{\mathrm{T}}|$ distribution for four different charged jet trigger momentum ranges from the top 20% events in V0A multiplicity from p–Pb collisions. The solid diamonds are the data points, while the open circles are from PYTHIA events simulated at the same $\sqrt{s_{\mathrm{NN}}}$. The bottom row of plots is the ratio of the data over the PYTHIA simulation from the top row.

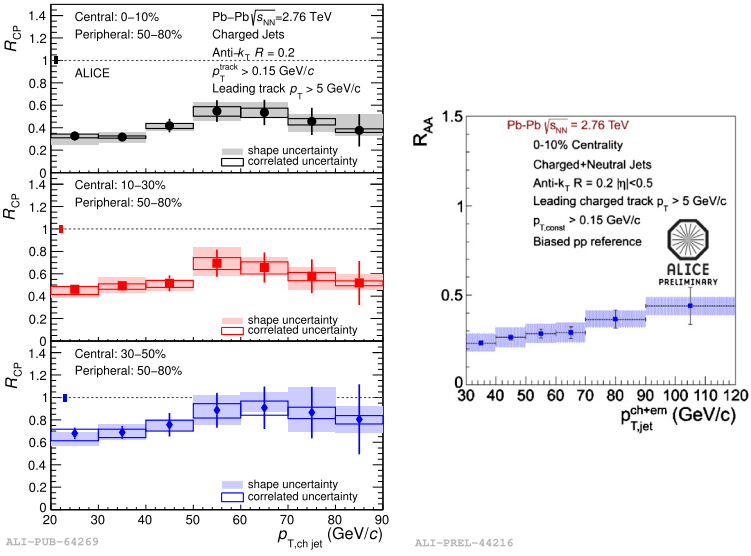

Fig. 4. The left figure shows R_{CP} for $R = 0.2$ charged jets with a leading track selection of $p_{\mathrm{T}} > 5$ GeV/c for three different centrality selections. For all three distributions, the reference spectrum is the result from 50–80% central events. The empty boxes indicate the correlated systematic uncertainty and the shaded boxes indicate the shape uncertainty [14]. On the right is R_{AA} for the 10% most central events for $R = 0.2$ jets with a leading track selection of $p_{\mathrm{T}} > 5$ GeV/c. The shaded boxes are the systematic uncertainties due to detector effects and unfolding added in quadrature with the systematics from Ref. [15].

transverse momentum than the trigger jet. By increasing the trigger jet transverse momentum, the kinematic reach of $|k_{\mathrm{T}}|$ is extended because this opens up phase-space for more radiation. The p–Pb data points and the PYTHIA8 simulation show a similar evolution with the p_{T} of the

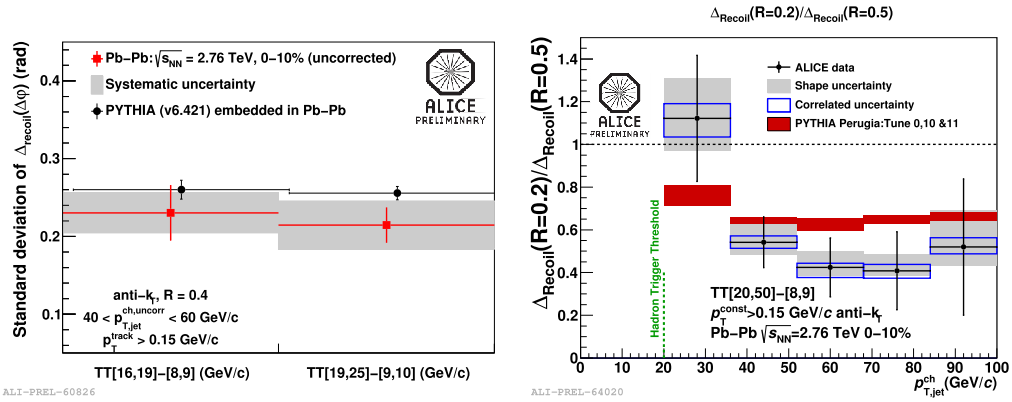

Fig. 5. The left figure shows the standard deviation of the width of subtracted hadron-jet azimuthal correlations for $R = 0.4$ jets from the 10% most central events in red squares and for PYTHIA events embedded in the data in black circles. The distribution of the left most point corresponds to the jet spectrum correlated with a trigger track between 16–19 GeV/c with the spectrum from 8 and 9 GeV/c subtracted from it. The right point is also the width of the recoiled jet distribution with the trigger track momentum selections of 19–25 GeV/c for the signal spectrum and 9–10 GeV/c for the reference. The right plot shows the subtracted recoil-jet distribution for the ratio of $R = 0.2$ jets over $R = 0.5$ jets from the 10% most central events in solid points. The shaded boxes are the shape uncertainty and the empty boxes are the correlated uncertainty. In the solid red boxes, the same distribution from PYTHIA is shown.

trigger jet, and the ratio of the two distributions is consistent with unity. No strong CNM are observed in p–Pb collisions in the measured kinematical region.

6. Results from Pb–Pb

One of the main experimental challenges in heavy-ion collisions is removing the contribution from the underlying events for the jet spectrum. As discussed in Section 5.1, this is done by determining the average background energy density event-by-event and subtracting it jet-by-jet [16,17]. The geometric background fluctuations were quantified by δp_T, which is considerably larger in central Pb–Pb collisions than it is in p–Pb. The smearing of the jet energy spectrum due to these background fluctuations, as well as the smearing due to detector effects, are corrected for in an unfolding procedure. For full jets it was necessary to require that all jets have a track with $p_T > 5$ GeV/c to achieve a stable result with the unfolding method. This selection is effective at removing combinatorial jets from the sample, without introducing a larger fragmentation bias of the signal jets [18].

The nuclear modification factor, R_{CP}, was calculated as the ratio of the charged jet yield in central collisions to the peripheral collisions, both contributions scaled by the number of binary collisions. In R_{CP} the reference spectrum should incorporate some of the CNM effects that could cause the nuclear modification factor to diverge from unity, however even in peripheral events the jet spectrum could still be modified by hot medium effects. In Fig. 4, we show R_{CP} for $R = 0.2$ charged jets from the 2010 Pb–Pb data for three different centrality selections as well as the nuclear modification factor for full jets, R_{AA}, [7]. In both analyses we found that jets are suppressed in central collisions, and that this suppression has a centrality dependence [14,15].

Another technique for measuring jets in Pb–Pb collisions is to use high p_T hadrons as triggers and then measure the away-side charged jets. This allows dijet events to be selected so that the signal-to-background ratio for the away side jets is larger. In addition, the trigger hadron will

be surface biased, which increases the average path-length that the away-side jets have traveled, so effects of the medium will be larger than for inclusive jets. A reference spectrum from a lower p_T trigger hadron can be subtracted from the signal spectrum to remove the combinatorial jet contribution in a model independent way. The advantage is that the fragmentation of the measured jets is not biased as it is with the leading track selection described above [19]. The charged jet spectra associated with the trigger track (TT) momentum ranges of 19–25, 16–19, 9–10 and 8–9 GeV/c were measured. One observable that was constructed was the hadron-jet azimuthal distribution $\Delta\phi = |\phi_{\text{trig}} - \phi_{\text{ch, jet}}|$. The width of this distribution was then compared to PYTHIA events embedded into minimum-bias Pb–Pb data. As seen in Fig. 5, the width of these distributions is consistent, indicating that there is no medium-induced jet deflection due to parton energy loss. In addition, the subtracted away-side spectra can be studied directly. The ratio of these spectra with different resolution parameters, similar to what was shown in the right plot in Fig. 1, can access the jet structure. As shown in Fig. 5, when compared to a PYTHIA model, there is a hint of energy redistribution but the results are consistent with no additional broadening within the current sizable statistical and systematic uncertainties.

7. Conclusions

ALICE has shown that the jet production mechanisms are well understood, with a variety of pp measurements at $\sqrt{s_{\text{NN}}} = 2.76$ and 7 TeV, which is important in establishing a baseline for cold nuclear and hot nuclear effects. In p–Pb collisions, we see no cold nuclear matter effects for the observables outlined in this proceedings. In Pb–Pb collisions jets are suppressed, with both R_{AA} and $R_{\text{CP}} < 1$. We also see that the suppression has a centrality dependence, with the largest suppression occurring in the most central events. From the azimuthal hadron-jet correlations, we see that even though jets are suppressed in central collisions, they are not significantly deflected.

References

[1] U.A. Wiedemann, Jet quenching in heavy ion collisions, arXiv:0908.2306.
[2] B.B. Abelev, et al., Performance of the ALICE experiment at the CERN LHC, arXiv:1402.4476.
[3] M. Cacciari, G.P. Salam, G. Soyez, The Anti-k(t) jet clustering algorithm, JHEP 0804 (2008) 063, http://dx.doi.org/10.1088/1126-6708/2008/04/063, arXiv:0802.1189.
[4] M. Cacciari, G.P. Salam, Dispelling the N^3 myth for the k_t jet-finder, Phys. Lett. B 641 (2006) 57–61, http://dx.doi.org/10.1016/j.physletb.2006.08.037, arXiv:hep-ph/0512210.
[5] M. Cacciari, G.P. Salam, Pileup subtraction using jet areas, Phys. Lett. B 659 (2008) 119–126, http://dx.doi.org/10.1016/j.physletb.2007.09.077, arXiv:0707.1378.
[6] M. Cacciari, J. Rojo, G.P. Salam, G. Soyez, Jet reconstruction in heavy ion collisions, Eur. Phys. J. C 71 (2011) 1539, http://dx.doi.org/10.1140/epjc/s10052-011-1539-z, arXiv:1010.1759.
[7] B. Abelev, et al., Measurement of the inclusive differential jet cross section in pp collisions at $\sqrt{s} = 2.76$ TeV, Phys. Lett. B 722 (2013) 262–272, http://dx.doi.org/10.1016/j.physletb.2013.04.026, arXiv:1301.3475.
[8] M. Vajzer, Charged jet spectra in proton–proton collisions with the ALICE experiment at the LHC, arXiv:1311.0148.
[9] B. Abelev, et al., Long-range angular correlations on the near and away side in p–Pb collisions at $\sqrt{s_{NN}} = 5.02$ TeV, Phys. Lett. B 719 (2013) 29–41, http://dx.doi.org/10.1016/j.physletb.2013.01.012, arXiv:1212.2001.
[10] M.L. Miller, K. Reygers, S.J. Sanders, P. Steinberg, Glauber modeling in high energy nuclear collisions, Annu. Rev. Nucl. Part. Sci. 57 (2007) 205–243, http://dx.doi.org/10.1146/annurev.nucl.57.090506.123020, arXiv:nucl-ex/0701025.
[11] R. Haake, Charged jets in minimum bias p–Pb collisions at $\sqrt{s} = 5.02$ TeV with ALICE, arXiv:1310.3612.
[12] T. Sjostrand, S. Mrenna, P.Z. Skands, PYTHIA 6.4 physics and manual, JHEP 0605 (2006) 026, http://dx.doi.org/10.1088/1126-6708/2006/05/026, arXiv:hep-ph/0603175.
[13] T. Sjostrand, S. Mrenna, P.Z. Skands, A brief introduction to PYTHIA 8.1, Comput. Phys. Commun. 178 (2008) 852–867, http://dx.doi.org/10.1016/j.cpc.2008.01.036, arXiv:0710.3820.

[14] B. Abelev, et al., Measurement of charged jet suppression in Pb–Pb collisions at $\sqrt{s_{NN}} = 2.76$ TeV, JHEP 1403 (2014) 013, http://dx.doi.org/10.1007/JHEP03(2014)013, arXiv:1311.0633.
[15] R. Reed, Full jet reconstruction in 2.76 TeV pp and Pb–Pb collisions in the ALICE experiment, J. Phys. Conf. Ser. 446 (2013) 012006, http://dx.doi.org/10.1088/1742-6596/446/1/012006, arXiv:1304.5945.
[16] B. Abelev, et al., Measurement of event background fluctuations for charged particle jet reconstruction in Pb–Pb collisions at $\sqrt{s_{NN}} = 2.76$ TeV, JHEP 1203 (2012) 053, http://dx.doi.org/10.1007/JHEP03(2012)053, arXiv:1201.2423.
[17] R.J. Reed, Inclusive jet spectra in 2.76 TeV collisions from ALICE, Nucl. Phys. A 904–905 (2013) 721c–724c, http://dx.doi.org/10.1016/j.nuclphysa.2013.02.116, arXiv:1211.5016.
[18] S. Aiola, Measurement of jet p_T spectra in Pb–Pb collisions at $\sqrt{s_{NN}} = 2.76$ TeV with the ALICE detector at the LHC, J. Phys. Conf. Ser. 446 (2013) 012005, http://dx.doi.org/10.1088/1742-6596/446/1/012005, arXiv:1304.6668.
[19] L. Cunqueiro, Jet structure in 2.76 TeV Pb Pb collisions at ALICE, Nucl. Phys. A 904–905 (2013) 728c–731c, http://dx.doi.org/10.1016/j.nuclphysa.2013.02.118, arXiv:1210.7610.